Video Article

Air Filter Devices Including Nonwoven Meshes of Electrospun Recombinant Spider Silk Proteins

Gregor Lang[1], Stephan Jokisch[1], Thomas Scheibel[1]

[1]Biomaterials Research Group, University of Bayreuth

Correspondence to: Thomas Scheibel at Thomas.Scheibel@fiberlab.de

Abstract

Based on the natural sequence of *Araneus diadematus* Fibroin 4 (ADF4), the recombinant spider silk protein eADF4(C16) has been engineered. This highly repetitive protein has a molecular weight of 48kDa and is soluble in different solvents (hexafluoroisopropanol (HFIP), formic acid and aqueous buffers). eADF4(C16) provides a high potential for various technical applications when processed into morphologies such as films, capsules, particles, hydrogels, coatings, fibers and nonwoven meshes. Due to their chemical stability and controlled morphology, the latter can be used to improve filter materials. In this protocol, we present a procedure to enhance the efficiency of different air filter devices, by deposition of nonwoven meshes of electrospun recombinant spider silk proteins. Electrospinning of eADF4(C16) dissolved in HFIP results in smooth fibers. Variation of the protein concentration (5-25% w/v) results in different fiber diameters (80-1,100 nm) and thus pore sizes of the nonwoven mesh.

Post-treatment of eADF4(C16) electrospun from HFIP is necessary since the protein displays a predominantly α-helical secondary structure in freshly spun fibers, and therefore the fibers are water soluble. Subsequent treatment with ethanol vapor induces formation of water resistant, stable β-sheet structures, preserving the morphology of the silk fibers and meshes. Secondary structure analysis was performed using Fourier transform infrared spectroscopy (FTIR) and subsequent Fourier self-deconvolution (FSD).

The primary goal was to improve the filter efficiency of existing filter substrates by adding silk nonwoven layers on top. To evaluate the influence of electrospinning duration and thus nonwoven layer thickness on the filter efficiency, we performed air permeability tests in combination with particle deposition measurements. The experiments were carried out according to standard protocols.

Video Link

The video component of this article can be found at http://www.jove.com/video/50492/

Introduction

Due to their combination of strength and extensibility, spider silk fibers can absorb more kinetic energy than most other natural or synthetic fibers [1]. Furthermore, unlike most synthetic polymeric materials silk materials are nontoxic and biocompatible and cause no allergic reaction when incorporated [2,3]. Putative health risks can be prevented by using spider silk. These features make spider silk highly attractive for a variety of medical and technical applications. Since spiders can't be farmed due to their cannibalistic behavior, biotechnological methods have been developed to produce spider silk proteins, both cost-efficiently and in sufficient quantities [4].

The recombinant silk protein eADF4(C16) has been engineered based on the natural sequence of *Araneus diadematus* Fibroin 4 (ADF4). eADF4(C16) has a molecular weight of 48kDa [5] and is soluble in various solvents (hexafluoroisopropanol (HFIP) [6], formic acid [7] and aqueous buffers) [8]. eADF4(C16) can be processed into different morphologies such as films [9], capsules [8], particles [10], hydrogels [11], coatings [7], fibers [12] and nonwoven meshes [6]. Due to their chemical stability, the latter provide high potential in filter applications.

Here, we present a protocol to fabricate air filter devices including a nonwoven mesh of electrospun recombinant spider silk proteins. Electrospinning or electrostatic spinning is a technique typically employed for producing polymer fibers with diameters in the range of 10 nm -10 μm [13], and nonwoven meshes have already been investigated for filter applications [14]. In the past, electrospinning has been successfully applied for processing of regenerated [15] as well as recombinantly produced [16] spider silk proteins. Typically a high electric voltage (5-30 kV) is applied to a syringe and a counter electrode (0-20 kV) placed in a distance of 8-20 cm. The strong electrostatic field induces repulsive forces within the charged solution. If the surface tension is exceeded, a Taylor cone is formed, and a thin jet erupts from the tip [17,18]. After formation, bending instabilities occur within the jet causing further stretching as the solvent evaporates, and a solid fiber is formed. Finally, the fiber is randomly deposited on the counter electrode as a nonwoven mesh [19]. Fiber properties like diameter and surface topology (smooth, porous) are mainly dependent on solution parameters such as concentration, viscosity, surface free energy and the solvent's intrinsic electrical conductivity and permeability [20]. Electrospinning of eADF4(C16) dissolved in HFIP results in smooth fibers with diameters from 80-1,100 nm depending on the protein concentration in the solution. eADF4(C16) electrospun from HFIP displays a predominantly α-helical secondary structure and the fibers

are water soluble [6]. In order to stabilize the silk fibers, β-sheet structures have to be induced by subsequent treatment with ethanol. In contrast to previously established post-treatment methods [21], in this study eADF4(C16) nonwovens have been treated with ethanol vapor in order to preserve the morphology of the silk fibers. Secondary structure analysis was performed using Fourier transform infrared spectroscopy (FTIR) and subsequent Fourier self-deconvolution (FSD) as described in the literature [22]. FSD is a signal-processing tool that allows resolution of FTIR spectra consisting of several overlapping bands. Thereby, the indistinct bands of the broad amid I region can be narrowed using a high pass filter to receive a deconvoluted spectrum with improved peak resolutions.

In order to evaluate the efficiency of filter substrates complemented with silk nonwoven meshes, air permeability tests were performed using an Akustron device according to standard protocols. Deposition rates were measured using a Palas universal particle sizer.

Protocol

1. Spinning Dope Preparation

1. Take lyophilized eADF4(C16) protein.
2. Weigh 20 mg of eADF4(C16) in a 1 ml reaction vessel by using a high precision scale.
3. Add 200 µl of hexafluoroisopropanol (HFIP) and seal the vessel with Parafilm.
   Note: HFIP is highly volatile and deleterious. As it can cause harm in the respiratory track, work under a safety hood, pipette carefully, and cap the tube.
4. Vortex the suspension for 1 min and further shake it to clear the solution. To ensure, that the entire amount of protein is completely dissolved, wait over-night.

2. Electrospinning

1. Prepare the electrospinning device (**Figure 1**): place the filter material on top of the counter electrode and preset the voltage of both the electrode (-22.5 kV) and the counter electrode (+2.5 kV). Set the volume flow to 315 µl/hr.
   Note: while electrospinning, toxic HFIP will be evaporated. Make sure your electrospinning device is connected to a fume hood.
2. Take a commercially available 20 G needle and grind the sharp tip with a hand grinder to a residual length of 30 mm. Connect the needle to a 1 ml syringe.
   Note: A plane needle tip is required in order to generate a well-defined Taylor cone.
3. Load the entire spinning dope (200 µl) into the syringe. Overlay the dope with 100 µl of air, in order to allow the complete solution to be extruded during the spinning process.
   Note: In order to avoid clogging of the needle, make sure that there are no particles (aggregates or impurities) in the spinning dope. Work under a fume hood!
4. Attach the filled syringe to the syringe pump of the electrospinning device and carefully press the piston onto the syringe until a droplet appears at the tip of the needle. Lock the piston.
5. Set the distance between the tip of the needle and the counter electrode to 8-20 cm.
6. Start the syringe pump and remove the (usually dried out) droplet from the opening of the needle. Activate all safety installations of the electrospinning device immediately and start the high voltage source as soon as a new droplet appears. Electrospinning of the spinning dope will start subsequently. Use a stopwatch to control spinning duration.
   Note: In order to avoid drying out of the solution and thus clogging of the needle, it is necessary to immediately start the spinning process after removing the dried droplet.
7. Since electrospinning of recombinant spider silk proteins depends on humidity and temperature, an adaptation of process parameters towards individual lab conditions might be necessary (**Figure 2**).
   Note: To prevent the droplet from drying (**Figure 2B**) enable a sufficient flow rate. If there is a low humidity in the surrounding atmosphere, adjust the relative humidity or raise the flow rate. Lower the voltage until a proper Taylor cone occurs (**Figure 2A**). When there is no solution at the tip (**Figure 2C**), raise the flow rate and lower the voltage until a droplet occurs. Then adjust voltage in order to establish a regular and stable Taylor Cone (**Figure 2A**).
8. After 30 sec / 60 sec / 90 sec of electrospinning switch off the syringe pump. In order to avoid falling droplets, wait 10 sec before turning off the high voltage source to release the residual pressure in the syringe.
9. Steps 6 to 8 can be performed on different types of filter materials, such as polyamide, polypropylene and polyester nonwoven meshes, as well as black paper for comparison.
10. To produce a nonwoven mesh for subsequent stability experiments, use black paper instead of filter material and perform steps 5 to 7. After 5 min of electrospinning, stop the process as described in step 8.

3. Post-treatment of Silk Nonwoven Meshes

1. Pre-heat an oven to 60 °C.
2. Place the filter substrates with eADF4(C16) nonwoven meshes vertically and with a minimum distance of 2 cm in a lockable glass container. The container should have two openings that will be used to subsequently introduce ethanol and water.
   Note: When fixing the filter materials, make sure that the area necessary for permeability experiments is not damaged by the clamps.
3. Connect two 60 ml syringes, one filled with ethanol and one filled with water, with silicone tubes pointing into the interior bottom of the post-treatment container (**Figure 3**).
   Note: In order to be able to remove the liquid from the container after the treatment, place the openings of the pipes as close as possible to the bottom.
4. Place the post-treatment container in the oven and add 60 ml of ethanol by extruding the syringe. Use a stopwatch to control treatment duration.

5. After 90 min of ethanol vapor treatment, remove the ethanol with the syringe from the glass, and add 60 ml of water from the second syringe.
6. Wait for another 90 min, then remove the water and switch off the oven. In order to avoid droplets by condensation, leave the container in the oven until it has completely cooled down.

4. Analysis of Spider Silk Nonwoven Meshes

1. Prepare the silk nonwoven meshes for stability tests on black paper or any other removable support. Cut two frames out of cardboard and adjust double-sticky adhesive tape. Press one frame onto the silk nonwoven mesh deposited on black paper and use a scalpel to cut off the excess of silk fibers (keep the excess fibers for subsequent SEM-imaging). Carefully remove the frame in order to detach the nonwoven from the paper. Repeat this step with the second frame (**Figure 4**).
2. Practical dip test: Cut a piece (1 cm^2) of each, the post-treated and non-treated silk nonwoven mesh and dip it into deionized water. The non-treated silk nonwoven mesh will immediately dissolve, while the treated nonwoven mesh will be stable (**Figure 5**). After dipping, dry the dipped sample and prepare it for SEM imaging.
3. Fourier transform infrared spectroscopy (FTIR)-measurement and subsequent Fourier self-deconvolution (FSD): In order to gain information about the structural changes of the silk proteins upon post-treatment of the nonwoven meshes, FTIR can be applied using the parameters: Transmittance-mode, scan from 800 to 4,000 cm^{-1}, 60 accumulations are measured and averaged for each spectrum, one reference is measured per spectrum. For quantitative analysis of the data, FSD can be employed (**Figure 6** and **Figure 7**). Thereby, the curves are reduced to the data area between 1,590 and 1,705 cm^{-1} and a baseline correction is performed. A local least square fit is calculated according to the peak positions taken from previous studies (1611, 1619, 1624, 1630, 1640, 1650, 1659, 1666, 1680, 1691, 1698 cm^{-1}) [22].
4. SEM imaging: SEM can be applied to investigate fiber diameters and the morphology of silk fibers on different filter substrates and to analyze the influence of the post-treatment on the fiber morphology (**Figure 8**). Use magnifications of 5,000x to 25,000x in order to get sufficiently detailed images.

5. Determination of Air Permeability

1. Place a proper fitting part of the filter material on the measuring area of an Akustron air permeability device. **Note:**: If you use another type of air permeability device, make sure that it fulfills the requirements of DIN 53 887, DIN 53 120, ISO 9237 and ASTM D 737-96 standards.
2. Employ an Akustron air permeability device (or any other as depicted in 5.1) . If necessary calculate the normed data [l / (m^2 x sec)].
3. Repeat steps 1 and 2 at least 10 times with different parts of your sample and calculate the arithmetic middle (**Figure 9**).
   Note: Measuring air permeability requires contact of the device and the nonwoven mesh. Thus, a careful handling of the samples is essential to prevent rupture of the delicate silk nonwoven mesh.

6. Determination of Filter Efficiency

1. Use a proper machine with pressure control and particle counter, such as a Universal particle sizer (Palas GmbH, Karlsruhe, Ger).
2. Place the filter samples in the device and measure particle retention (**Figure 10**). Aerosol: Di-ethyl-hexyl-sebacat (DEHS); particle sizes: 0.3-3 µm; duration: 30 sec; liquid velocity: 2,350 cm/sec; air flow: 3,400 m^3/hr.
   Note: Handle the sample with care and do not touch the surface to prevent destruction of the nonwoven mesh and avoid any pollution. Be sure to create enough samples of equal quality for performance measurements.

Representative Results

Electrospinning of recombinant spider silk solutions with concentrations of 10% w/v from HFIP resulted in smooth fibers with diameters ranging from 80 to 120 nm, allowing the formation of nonwoven meshes. Post-treatment with ethanol vapor did not lead to conspicuous morphological changes, which was, therefore, established as a proper way of silk nonwoven post-treatment (**Figure 8**). Structural changes were detected using FT-IR and subsequent FSD of amid I bands was performed to analyze single contribution peaks (**Figure 6**). It could be shown that post-treatment leads to an increase in β-sheet structures, while the content of α-helical und random coil structures decreases (**Figure 7**). This result can be practically proven by dipping a post-treated nonwoven into water (**Figure 5**). Even after one week, no dissolution of the nonwoven mesh will occur.

The spinning duration is the most important parameter concerning the application of silk nonwovens in filter materials due to the pressure drop based on the increasing density of electrospun fibers. Extended spinning durations und thus a higher number of fiber layers result in an exponential decrease of air permeability. This effect could be detected for all different filter substrate materials before and after post-treatment (**Figure 9**). Likewise, the filtering efficiency of the silk-containing filter materials of sub-micrometer particles increases (**Figure 10**). While short spinning durations (30 sec) gain low filter efficiencies, higher spinning durations (90 sec) lead to higher efficiencies.
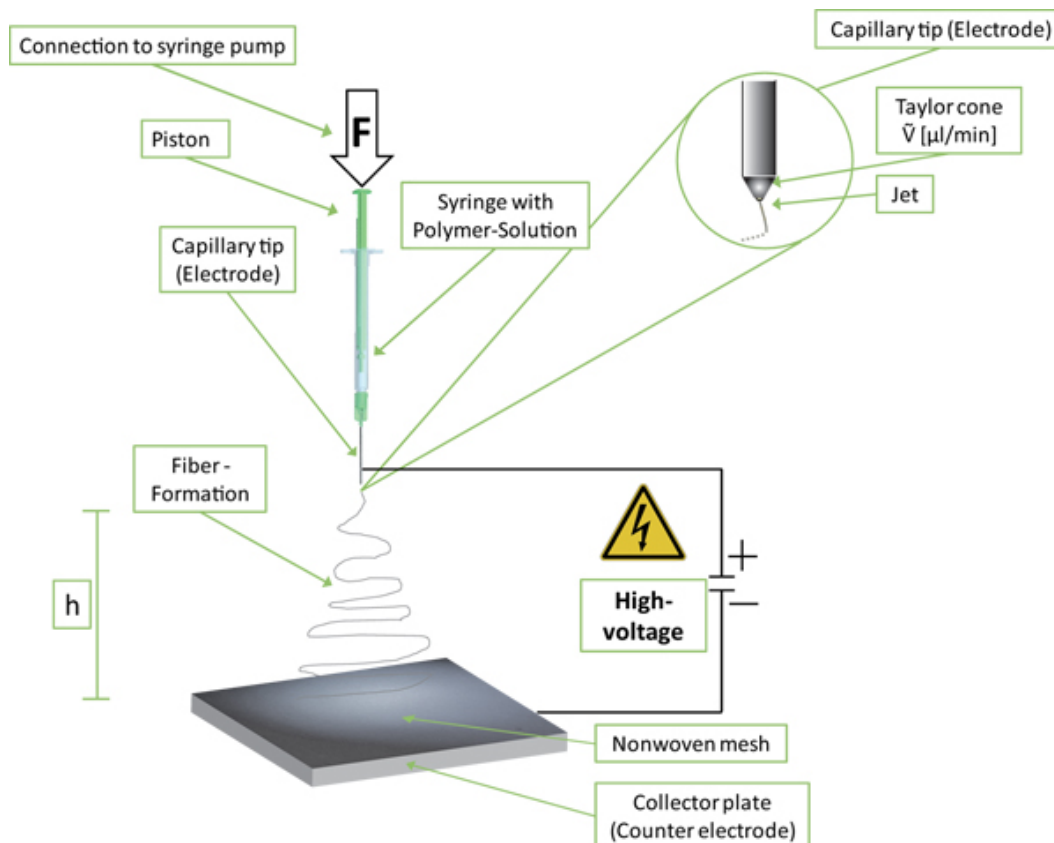
Figure 1. High electric voltage (0-30 kV) is applied to a syringe filled with a silk solution, and a counter electrode (0-20 kV) is placed in a distance of 8-20 cm. This setup leads to a strong electrostatic field, inducing repulsive forces within the charged solution. If the surface tension is exceeded, a Taylor cone is formed, and a thin jet erupts from the tip. After formation, bending instabilities occur within the jet causing further stretching as the solvent evaporates, and a solid fiber is formed. Finally, the fiber is randomly deposited on the counter electrode in the form of a nonwoven mesh.
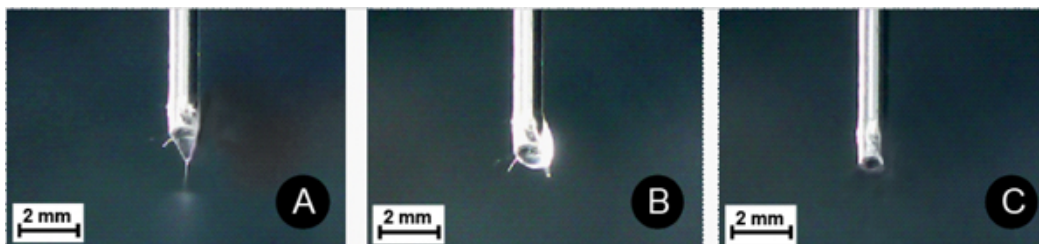
Figure 2. Photographs of a regular Taylor cone **(A)**, a dried droplet **(B)**, and the setup without droplet **(C)**.
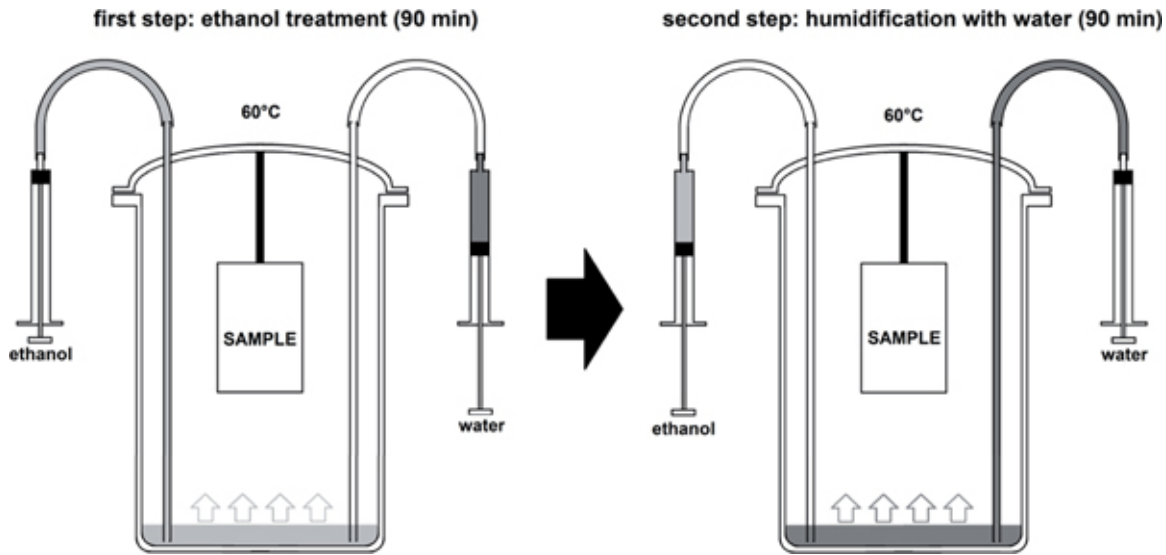
Figure 3. Schematic procedure during vapor post-treatment. In the first step, the chamber is filled with ethanol, and the sample is steamed at 60 °C for 90 min. In order to soften the nonwoven meshes for subsequent handling, ethanol is removed and the fibers are steamed with water vapor for 90 min at 60 °C. Click here to view larger figure.
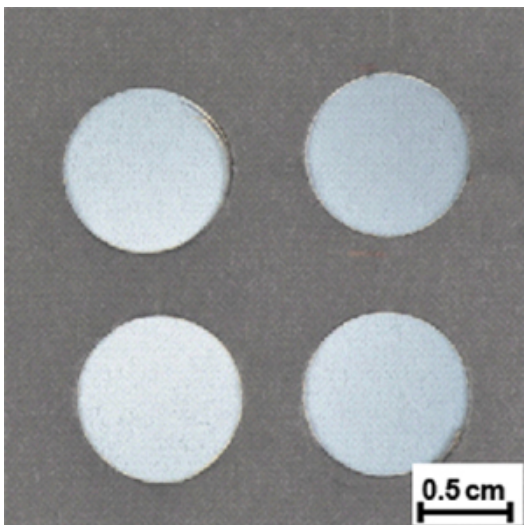

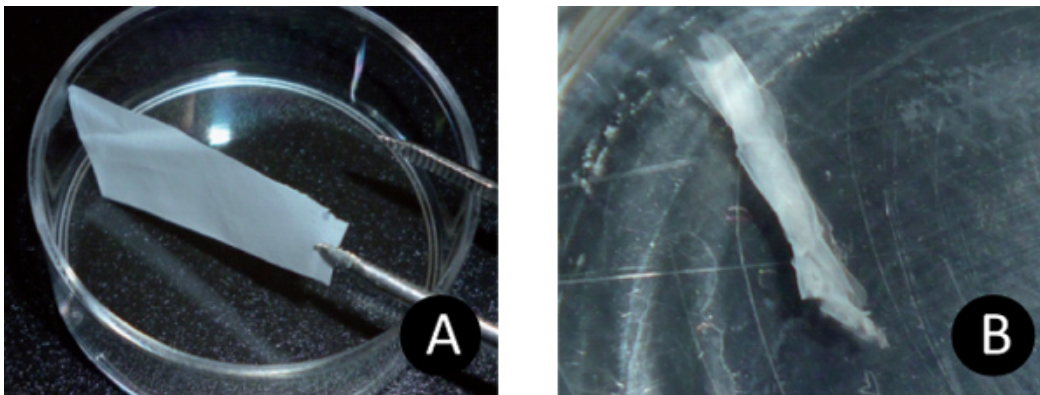**Figure 4.** Photograph of a cardboard frame with attached silk nonwoven meshes to be used for post-treatment.

Figure 5. Electrospun and subsequently post-treated nonwoven in dry state **(A)** and under water **(B)**.
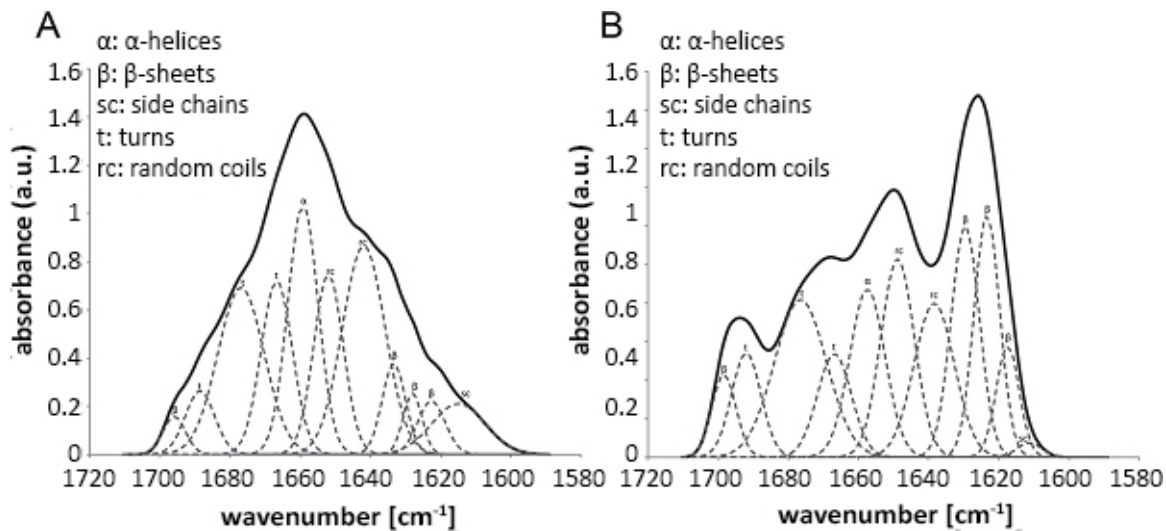
Figure 6. Fourier self-deconvoluted absorbance spectrum of an amide I band of an untreated **(A)** and a post-treated **(B)** spider silk nonwoven mesh. The solid line displays the absorbance band resulting from the single contribution peaks (dotted lines) as derived after deconvolution. The assignment of the respective curves was based on previously published values from the literature [22]. Click here to view larger figure.
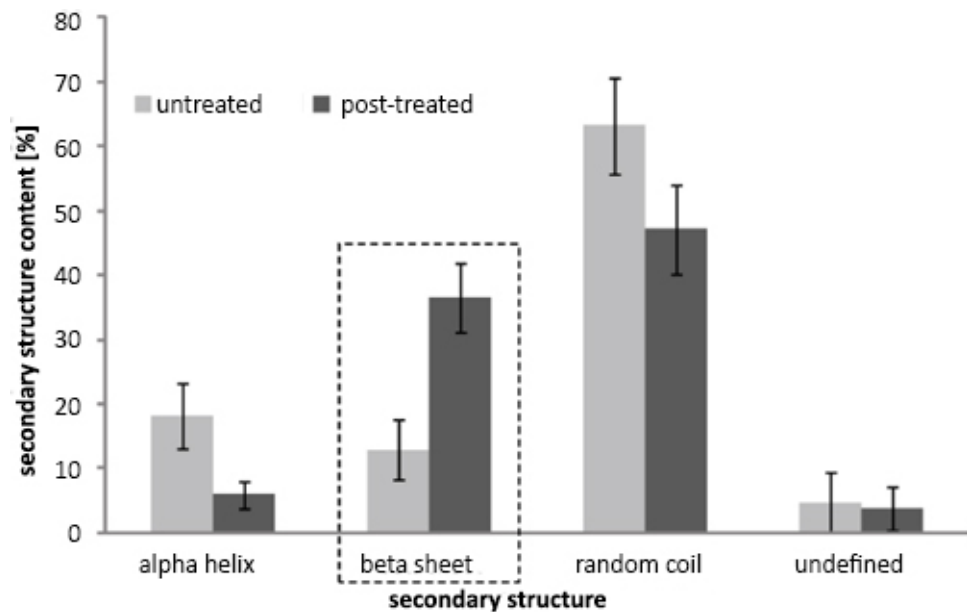

Figure 7. Secondary structure content of non-treated and post-treated eADF4(C16) nonwoven meshes.
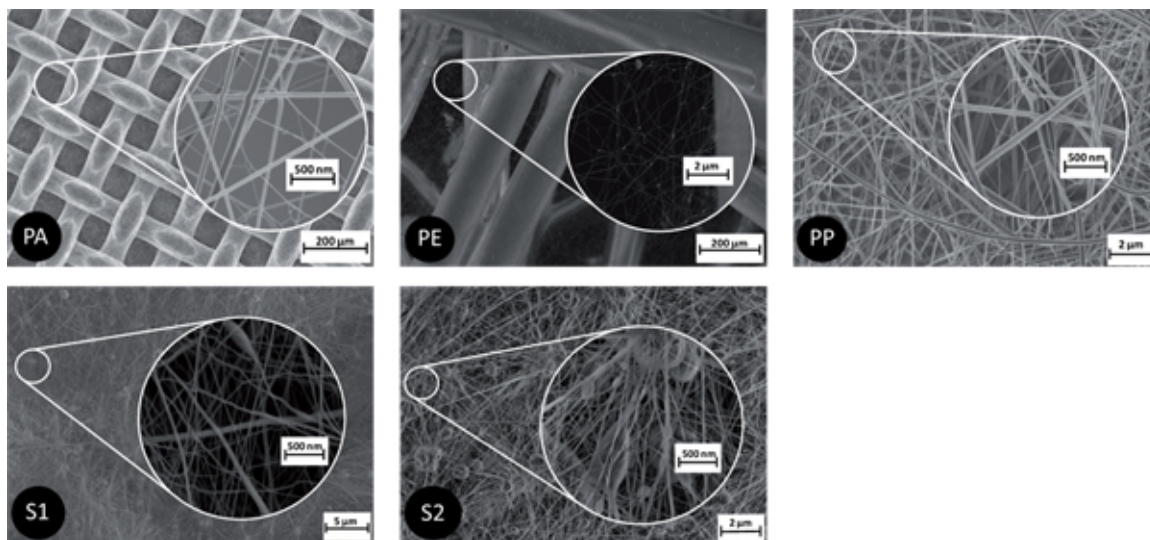
Figure 8. SEM images of electrospun eADF4(C16)-fibers on different filter substrates: Polyamide (PA), Polyester (PE), Polypropylene (PP) and pure eADF4(C16) fibers before (S1) and after (S2) post-treatment with ethanol vapor. Click here to view larger figure.
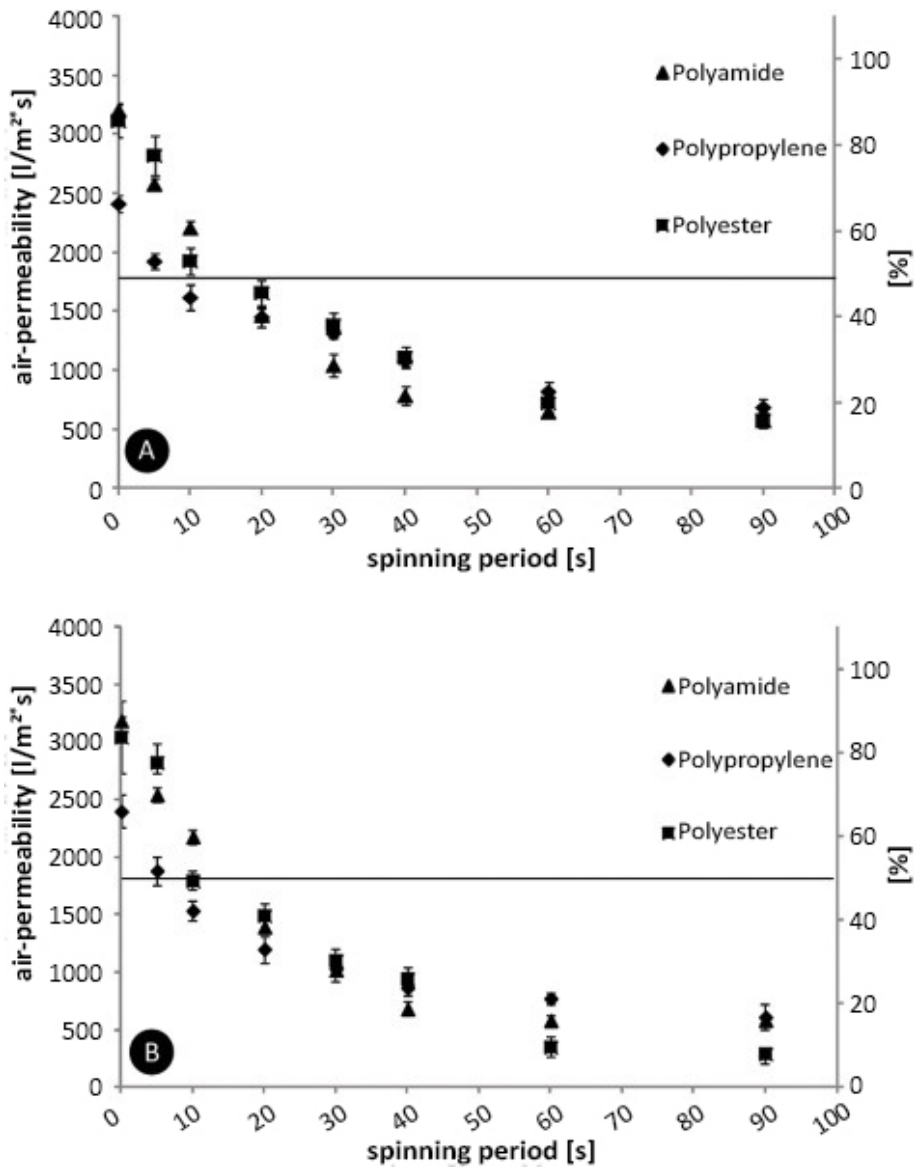
Figure 9. Air permeability tests, before **(A)** and after post-treatment **(B)** of the silk nonwoven meshes with ethanol vapor, increasing spinning times lead to more nonwoven layers subsequently lowering the air permeability.
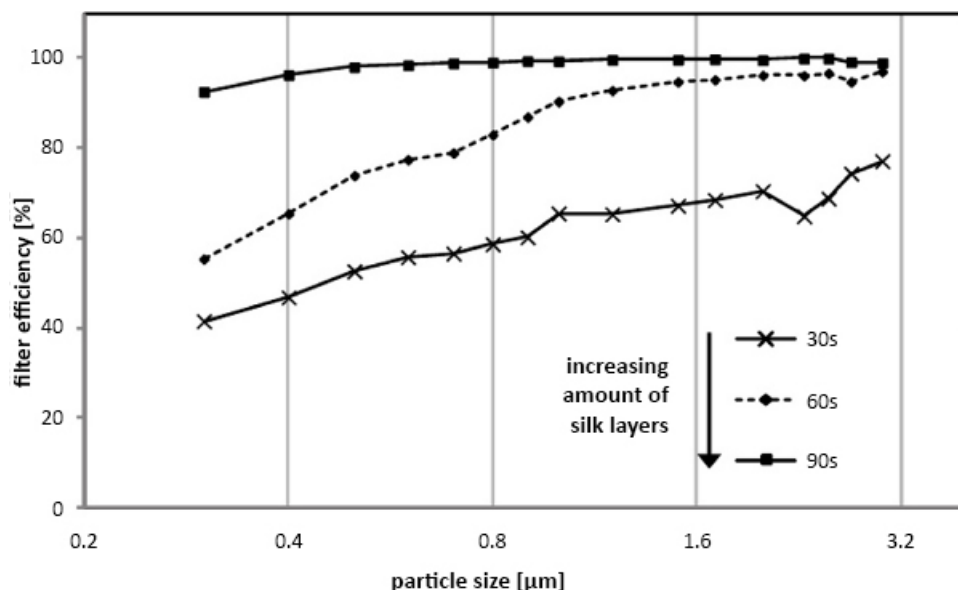
Figure 10. Filter efficiency of di-ethyl-hexyl-sebacat aerosol on electrospun spider silk nonwoven meshes on polyamide filter materials at different spinning durations, influencing the silk layer quantity, after post-treatment with ethanol.

Discussion

New filter devices should allow lowering the overall energy consumption in air filtration at constant or higher filter efficiencies. Here, such devices were created using nonwovens made of spider silk. Due to its low surface tension and high volatility, HFIP has been chosen as a suitable solvent for the electrospinning process. Furthermore, aqueous silk solutions have been tested in previous experiments, but no fibers could be generated. Here, it would be crucial to use additives in order to lower the surface tension and thereby improve the spinning properties of the solution. The most critical step is to adjust the conditions and the used material concentration and solvent of the spinning solution, spinning height, voltage and extrusion velocity. During performance, for instance clogging of the tip can be prevented by supplying the needle tip with moisture in form of water vapor, but any kind of additions in the electrospinning setup might subsequently disturb the sensitive process and electric field. Essential process parameters (concentration, voltage, distance, humidity) were individually determined carrying out separate experimental series (data not shown). Taking all parameters into consideration it is crucial to take care of a continuous taylor cone and spinning process to create uniform fibers.

The filter efficiency is one of the most important parameters of filter materials. This parameter is mainly influenced by the structure of the filter material. Wovens inherit uniform pore sizes and subsequently consistent air permeability. It is crucial to create homogeneous nonwoven meshes on these template materials to fill the pores and to generate a zero-defect filter. The filter efficiency in our filters shows a direct dependence on the spinning duration (of the silk proteins), and, therefore, on the number of nonwoven mesh layers. The gaps between single fibers are consistently filled, enabling the retention of smaller particles.

In this work we introduced a method to produce a novel filter material with spider silk nonwoven meshes, showing high filter efficiency. Therefore, these filters are promising candidates for future usage in air filtration systems.

Disclosures

We have nothing to disclose.

Acknowledgements

References

1. Gosline, J.M., Guerette, P.A., Ortlepp, C.S., & Savage, K.N. The mechanical design of spider silks: From fibroin sequence to mechanical function. *J. Exp. Biol.* **202**, 3295-3303 (1999).
2. Vollrath F, B.P., Basedow A, Engström W, & List H. Local tolerance to spider silks and protein polymers *in vivo. In Vivo.* **16**, 229-234 (2002).
3. Allmeling, C., *et al.* Spider silk fibres in artificial nerve constructs promote peripheral nerve regeneration. *Cell Prolif.* **41**, 408-420 (2008).
4. Huemmerich, D., Helsen C.W., *et al.* Primary structure elements of spider dragline silks and their contribution to protein solubility. *Biochemistry.* **43**, 13604-13612 (2004).

May 2013 | 75 | e50492 | Page 9 of 10

5. Huemmerich, D., Slotta, U., & Scheibel, T. Processing and modification of films made from recombinant spider silk proteins. *Appl. Phys. a-Mater.* **82**, 219-222 (2006).
6. Leal-Egana, A., Lang, G., *et al.* Interactions of Fibroblasts with Different Morphologies Made of an Engineered Spider Silk Protein. *Adv. Eng. Mater.* **14**, B67-B75 (2012).
7. Wohlrab, S., Spiess, K., & Scheibel, T. Varying surface hydrophobicities of coatings made of recombinant spider silk proteins. *J. Mater. Chem.* **22**, 22050-22054 (2012).
8. Hermanson, K.D., Huemmerich, D., Scheibel, T., & Bausch, A.R. Engineered microcapsules fabricated from reconstituted spider silk. *Adv. Mater.* **19**, 1810-1815 (2007).
9. Spiess, K., Wohlrab, S., & Scheibel, T. Structural characterization and functionalization of engineered spider silk films. *Soft Matter.* **6**, 4168-4174 (2010).
10. Slotta, U.K., Rammensee, S., Gorb, S., & Scheibel, T. An engineered spider silk protein forms microspheres. *Angew. Chem.-Int. Edit.* **47**, 4592-4594 (2008).
11. Schacht, K. & Scheibel, T. Controlled hydrogel formation of a recombinant spider silk protein. *Biomacromolecules.* **12**, 2488-2495 (2011).
12. Exler, J.H., Hummerich, D., & Scheibel, T. The amphiphilic properties of spider silks are important for spinning. *Angew. Chem.-Int. Edit.* **46**, 3559-3562 (2007).
13. Sundaray, B., Subramanian, V., *et al.* Electrospinning of continuous aligned polymer fibers. *Appl. Phys. Lett.* **84**, 1222-122, (2004).
14. Van Hulle, S.W. H.,Bjorge, D., *et al.* Performance assessment of electrospun nanofibers for filter applications. *Desalination.* **249**, 942-948 (2009).
15. Zhou, S.B.,Peng, H.S., *et al.* Preparation and characterization of a novel electrospun spider silk fibroin/poly(D,L-lactide) composite fiber. *J. Phys. Chem. B.* **112**, 11209-11216 (2008).
16. Stephens, J.S., Fahnestock, S.R., *et al.* Effects of electrospinning and solution casting protocols on the secondary structure of a genetically engineered dragline spider silk analogue investigated via fourier transform Raman spectroscopy. *Biomacromolecules.* **6**, 1405-1413 (2005).
17. Greiner, A. & Wendorff, J.H. Electrospinning: a fascinating method for the preparation of ultrathin fibers. *Angew. Chem.-Int. Edit.* **46**, 5670-5703 (2007).
18. Smit, E., Buttner, U., & Sanderson, R.D. Continuous yarns from electrospun fibers. *Polymer.* **46**, 2419-242, (2005).
19. Teo, W.E. & Ramakrishna, S. A review on electrospinning design and nanofibre assemblies. *Nanotechnology.* **17**, R89-R106 (2006).
20. Greiner, A., Wendorff, J.H., Yarin, A.L., & Zussman, E. Biohybrid nanosystems with polymer nanofibers and nanotubes. *Appl. Microbiol. Biotechnol.* **71**, 387-393 (2006).
21. Spiess, K., Lammel, A., & Scheibel, T. Recombinant spider silk proteins for applications in biomaterials. *Macromolecular Biosciences.* **10**, 998-1007 (2010).
22. Hu, X., Kaplan, D., & Cebe, P. Determining beta-sheet crystallinity in fibrous proteins by thermal analysis and infrared- spectroscopy. *Macromolecules.* **39**, 6161-6170 (2006).